OPEN

The Compressed Sensing MP2RAGE as a Surrogate to the MPRAGE for Neuroimaging at 3 T

Aurélien J. Trotier, PhD, Bixente Dilharreguy, PhD,† Serge Anandra, MS,† Nadège Corbin, PhD,*‡ William Lefrançois, PhD,* Valery Ozenne, PhD,* Sylvain Miraux, PhD,* and Emeline J. Ribot, PhD**

Objectives: The magnetization-prepared 2 rapid acquisition gradient echo (MP2RAGE) sequence provides quantitative T_1 maps in addition to high-contrast morphological images. Advanced acceleration techniques such as compressed sensing (CS) allow its acquisition time to be compatible with clinical applications. To consider its routine use in future neuroimaging protocols, the repeatability of the segmented brain structures was evaluated and compared with the standard morphological sequence (magnetization-prepared rapid gradient echo [MPRAGE]). The repeatability of the T_1 measurements was also assessed.

Materials and Methods: Thirteen healthy volunteers were scanned either 3 or 4 times at several days of interval, on a 3 T clinical scanner, with the 2 sequences (CS-MP2RAGE and MPRAGE), set with the same spatial resolution (0.8-mm isotropic) and scan duration (6 minutes 21 seconds). The reconstruction time of the CS-MP2RAGE outputs (including the 2 echo images, the MP2RAGE image, and the T_1 map) was 3 minutes 33 seconds, using an open-source in-house algorithm implemented in the Gadgetron framework.

Both precision and variability of volume measurements obtained from CAT12 and VolBrain were assessed. The T_1 accuracy and repeatability were measured on phantoms and on humans and were compared with literature.

Volumes obtained from the CS-MP2RAGE and the MPRAGE images were compared using Student *t* tests ($P < 0.05$ was considered significant).

Results: The CS-MP2RAGE acquisition provided morphological images of the same quality and higher contrasts than the standard MPRAGE images. Similar intravolunteer variabilities were obtained with the CS-MP2RAGE and the MPRAGE segmentations. In addition, high-resolution T_1 maps were obtained from the CS-MP2RAGE. T_1 times of white and gray matters and several deep gray nuclei are consistent with the literature and show very low variability (<1%).

Conclusions: The CS-MP2RAGE can be used in future protocols to rapidly obtain morphological images and quantitative T_1 maps in 3-dimensions while maintaining high repeatability in volumetry and relaxation times.

Key Words: MP2RAGE, compressed sensing, MPRAGE, volumetry, T_1 mapping, repeatability

(*Invest Radiol* 2022;57: 366–378)

Received for publication September 3, 2021; and accepted for publication, after revision, November 8, 2021.

From the *Centre de Résonance Magnétique des Systèmes Biologiques, UMR5536, CNRS/Université de Bordeaux, and †Biomedical Imaging Facility (pIBIO), UMS3767, CNRS/Université de Bordeaux, Bordeaux, France; and ‡UCL Queen Square Institute of Neurology, Wellcome Centre for Human Neuroimaging, University College of London, London, United Kingdom.

Conflicts of interest and sources of funding: None of the authors have any conflict of interest to declare. This study was achieved within the context of the Laboratory of Excellence TRAIL ANR-10-LABX-57. This work was also supported by the French National Research Agency (ANR-19-CE19-0014).

Correspondence to: Emeline J. Ribot, PhD, Centre de Résonance Magnétique des Systèmes Biologiques, 146 Rue Léo Saignat, 33076 Bordeaux, France. E-mail: ribot@rmsb.u-bordeaux.fr.

Supplemental digital contents are available for this article. Direct URL citations appear in the printed text and are provided in the HTML and PDF versions of this article on the journal's Web site (www.investigativeradiology.com).

Copyright © 2022 The Author(s). Published by Wolters Kluwer Health, Inc. This is an open-access article distributed under the terms of the Creative Commons Attribution-Non Commercial-No Derivatives License 4.0 (CCBY-NC-ND), where it is permissible to download and share the work provided it is properly cited. The work cannot be changed in any way or used commercially without permission from the journal.

ISSN: 0020-9996/22/5706–0366
DOI: 10.1097/RLI.0000000000000849

Quantitative biomarkers are more often used for diagnostic, prognostic, and predictive purposes.[1,2] In magnetic resonance imaging (MRI), one of the most intrinsic biomarkers is tissue relaxation times. For instance, the longitudinal relaxation time T_1 has great value in various applications. It has been shown to be influenced by age,[3–5] to be correlated with myelin content,[6,7] to reflect cortical microstructural modifications in multiple sclerosis, Parkinson disease, and epileptic patients,[8–10] to be influenced by oxygen level,[11] and to be a biomarker of chemotherapies.[12] Recently, a study demonstrated that quantitative T_1 mapping might be more sensitive than conventional T_1-weighted imaging to detect infiltration of glioma cells.[13] Consequently, high spatial resolution mapping of this quantitative measurement has an increasing interest. Nevertheless, both availability and diversity of MR sequences and reconstruction methods slow down the clinical evaluation and acceptability. Thus, there has been a deep focus on the reproducibility in the quantitative measurements (ISMRM reproducibility challenge 2020: https://blog.ismrm.org/2019/12/12/reproducibility-challenge-2020-join-the-reproducible-research-and-quantitative-mr-study-groups-in-their-efforts-to-standardize-t1-mapping) to use this parameter at a broader scale.

Among the MR sequences used for T_1 mapping, the magnetization-prepared 2 rapid acquisition gradient echo (MP2RAGE) is getting huge interest in research settings due to both the high contrasts it generates at magnetic fields higher than 1.5 T and the ability to obtain T_1 maps with high spatial resolution because of the 3-dimensional (3D) encoding scheme. In addition, due to a specific combination of the 2 gradient echo (GRE) images acquired at 2 different inversion times, inhomogeneity of the receive B_1^- field is canceled,[14] which is an interesting property when combining large amounts of phased array coils. Nevertheless, due to the inherent delays within the sequence, the relatively long acquisition time remains a problem for routine application in clinics. Some research teams used theses dead times to lengthen the GRE blocks. Through multiecho acquisitions, other parametric information such as T_2*[15] and magnetic susceptibility[16,17] were simultaneously measured. In parallel, modifying the encoding into an echo planar encoding enabled to fasten acquisition times by a factor of approximately 4 compared with the conventional MP2RAGE.[18] Such long echo planar GRE blocks could affect signal-to-noise ratio (SNR) due to TE lengthening, are prone to distortion artifact, could generate T_1 blurring limiting the detection of thin structures, and might increase the sensitivity to transmit B1 due to higher flip angles.

In the last years, the compressed sensing (CS) acceleration technique is getting tremendous interests. This technique has been combined with the MP2RAGE sequence at 7 T to obtain mouse brain T_1 maps in less than 3 minutes.[19] In addition, a recent study has combined it with the MP2RAGE sequence at 3 T for human neuroimaging.[20] Acceleration by a factor of 5 did not affect the volume measurements of several brain structures compared with the conventional GRAPPA-accelerated MP2RAGE sequence. Furthermore, the CS technique enables to increase the acceleration factor without affecting SNR as much as with parallel imaging acceleration.[21] To implement the CS technique within the MP2RAGE sequence, specific encoding trajectories had to be implemented, such as the variable density Poisson[19] or a disk-shaped mask.[20] The subsequent reconstruction durations are usually time-consuming.

Consequently, rapid acquisition must be combined with fast reconstruction algorithms compatible with clinical constraints. Although this information is crucial before any translation to clinics, no information on that processing was mentioned previously when applying the CS-MP2RAGE on humans.

In addition, to use the CS-accelerated version of the MP2RAGE into clinical protocols and potentially replace the morphological magnetization-prepared rapid gradient echo (MPRAGE) sequence, further investigation is required. The MPRAGE sequence is used in protocols of many neuroimaging studies as an anatomical reference. For example, it is used in clinical multiple sclerosis protocols,[22] in the Alzheimer's Disease Neuroimaging Initiative, and the Human Connectome protocols with high spatial resolution, greater than 1 mm. Indeed, "deep brain regions" (ie, the thalamus, globus pallidus, caudate, and putamen) are treatment targets for a variety of functional disorders, and given their anatomical complexity, an isotropic spatial resolution of more than 1 mm^3 is desirable for imaging these regions.

Nevertheless, none of the 2 studies that developed the CS-MP2RAGE assessed its efficiency and compared it with the MPRAGE sequence, although the CS-MP2RAGE sequence has the potential to give similar information than the MPRAGE, and in addition provide a T_1 map.

Consequently, the goal of this study is to fill this lack of information to complete the last steps toward the potential routine clinical implementation of the CS-MP2RAGE.

Thus, for the same acquisition time, the objective was to obtain, with the MP2RAGE sequence, at least the same accuracy in terms of brain structure segmentation and corresponding volumes estimation as the MPRAGE sequence, while providing additional quantitative information (T_1 values) with high repeatability over repeated independent examinations. Indeed, a high repeatability and accuracy of the T_1 measurements are mandatory for longitudinal studies.

Consequently, we designed an MP2RAGE sequence compatible with CS acceleration, available on a 3 T MRI scanner and that rapidly reconstructs 3D T_1 maps, without the user noticing the multiple steps of the reconstruction process. This method enabled to reach a protocol of less than 10 minutes (including the acquisition duration of 6 minutes 21 seconds and the fast reconstruction time of 3 minutes 33 seconds) for high spatial resolution (0.8-mm isotropic) T_1 mapping.

The volumes of several brain tissues and subcortical gray nuclei of healthy volunteers were compared between the MPRAGE and the MP2RAGE sequences, using widely used segmentation tools. The repeatability of the sequences was quantified for both volumetric and T_1 measurements and compared with literature. We thus assessed if the CS-MP2RAGE protocol could replace the standard morphological MPRAGE images in clinics.

MATERIALS AND METHODS

Magnetic Resonance Imaging Acquisitions

The experiments have been performed on a 3 T Prisma Siemens scanner using a body coil for transmission and a 64-channel head coil for signal reception.

Protocol

The CS-MP2RAGE sequence was performed using isotropic voxels of 0.8 mm^3 (field of view [FOV], 256 × 256 × 192 mm; matrix, 320 × 320 × 240). The other parameters were as follows: echo train length (ETL), 125; echo time/repetition time [TE/TR], 3.5/7 milliseconds; $\alpha1/\alpha2$, 7/7 degrees; TI1/TI2/MP2RAGE_TR, 800/2200/5000 milliseconds (see Supplementary Figs. 1–2, http://links.lww.com/RLI/A666 for more details). The same CS pattern as in Trotier et al[19] has been implemented. Shortly, it is based on the reordering of a variable density Poisson mask (adapted from an initial implementation of Lustig et al[23] in the SPARSE MRI Toolbox to sample the k-space from bottom to top for each echo train; see Fig. 1 in Trotier et al[19]). The central part of the k-space is fully sampled to form a square along ky/kz with a dimension 24 × 24. Those lines are used during the reconstruction pipeline to estimate the coil sensitivity maps. This encoding does not require that the length of the echo train is equal to the number of partitions along the kz-axis (slice partitions). This enables more flexibility in the choice of contrasts and geometric parameters. Although the same FOV and matrices were used throughout our whole study, this flexibility can be used to adapt the FOV size to each participant without affecting the ETL length (maintaining the contrast, a low T_1 blurring, and thus the accuracy in the T_1 measurements). An acceleration of CS factor 8.06 (noted CS8 thereafter) was performed for each acquisition to match the duration of the corresponding MPRAGE acquisitions (acquired with the same spatial resolution [0.8 mm^3]; TI, 1070 milliseconds; ETL in the slice direction, 240; MPRAGE_TR, 2120 milliseconds; TE/TR, 2.35/8.7 milliseconds; α, 9 degrees; GRAPPA2). This latter protocol is routinely performed in our center.[24,25] Each sequence lasted 6 minutes 21 seconds. The MPRAGE sequence was considered as the criterion standard for the volumetric measurements.

Phantom Study

A phantom containing 8 tubes filled with 1.5% agarose and increasing concentrations of Gd-DOTA (DOTAREM, Guerbet, France) from 0.01 mM to 0.3 mM was built to create a large range of T_1 values, including values outside those of the healthy brains. This phantom was remade 2 times. The following experiment was thus performed 3 times independently. Data were acquired with 3 different protocols in each session: the proposed CS8-MP2RAGE sequence, the vendor MP2RAGE sequence either fully sampled (21 minutes 22 seconds) or accelerated through parallel imaging with a factor of 3 (8 minutes 27 seconds, as described and validated in the initial MP2RAGE publication[14]). For these latter sequences, the following parameters were used: ETL, 176; TE/TR, 3.5/7 milliseconds; $\alpha1/\alpha2$, 4/5 degrees; TI1/TI2/MP2RAGE_TR, 800/2200/5000 milliseconds; and the vendor dedicated reconstruction was used.

Volunteers

In total, 13 volunteers (aged between 26 and 31 years, 3 female) were scanned 3 or 4 times at different days of interval, with approval granted by the local ethics committee and the informed written consent of the participants. The study was approved by the regional French Human Protection Committee (CPP 2016/20 2016-A00434-47). Each session included the proposed CS8 protocol and the criterion standard MPRAGE protocol.

Reconstruction Process

The reconstruction pipeline has been implemented on the open-source Gadgetron software, which is getting widely used due to its flexibility, fast processing, and the large gallery of scripts enabling to reconstruct images with nonconventional encoding strategies.[26] Acquisition data sets are automatically sent to Gadgetron (version 4.1) on an external station (2 processors Intel Xeon E52640 V4 [10C, 2.43.4 GHz, 25Mo, 9 W/C, 2133 MHz] with 128Go 2400 MHz DDR4 and 2 Nvidia Quadro P5000 of 16Go).

The house-made reconstruction code is using the Berkeley Advanced Reconstruction Toolbox (BART, version 0.6.0) with Matlab and is fully integrated in Gadgetron as a "gadget."

The reconstruction pipeline is encapsulated in a docker image for interscanner and intersite reproducibility purpose and is available in this GITHUB repository (https://github.com/CRMSB/PAPER_MP2RAGE_CS).

The image reconstruction pipeline is as follows:

1. Each raw data line is sent to Gadgetron, coil-compressed to 12 virtual coils, then buffered in Matlab to form the undersampled k-space.
2. Sensitivity coil maps are generated using the central part of the TI2 k-space.[27]

© 2022 The Author(s). Published by Wolters Kluwer Health, Inc.

3. A joint parallel imaging and CS reconstruction ("pics" function in BART) with the same wavelet regularization parameters for both TI1 and TI2 images is applied. This function solves the following problem using a FISTA algorithm[28]:

$$\hat{m} = \underset{m}{\operatorname{argmin}} \frac{1}{2} \| PFCm - y \|_2^2 + \lambda \| Wm \|_1$$

with m being the image estimates, y the undersampled k-space, P the binary sampling mask, F the discrete Fourier transform, λ the regularization parameter, and W the wavelet transform.

4. The 2 images are combined to generate the MP2RAGE image and T_1 maps using a lookup table computed from the acquisition parameters.[14]
5. Using the Gadgetron software, the TI1 and TI2 images, the MP2RAGE image without the salt-and-pepper background (not shown here), and the easily interpretable jet-colored T_1 map are sent to the MR console. This enables an easy and rapid checkup before any postprocessing. This process is totally imperceptible to the user.

Regularization parameters for the CS reconstruction were empirically optimized and set to $\lambda = 0.01$ with 30 iterations corresponding to a total reconstruction time of 3 minutes 33 seconds only.

It is important to note that, as the reconstruction pipeline occurs on a separate workstation, other complementary acquisitions can be performed during this time lapse.

Image Analysis

As mentioned earlier, commonly-used softwares were used here to segment the brain structures from both the MPRAGE and the MP2RAGE images, to limit analysis bias, and to accommodate to a large community of potential users and multiple MR vendors.

First, segmentation of brain white matter (WM), gray matter (GM), and cerebrospinal fluid (CSF) was performed using the well-established pipeline of the Computational Anatomy Toolbox (CAT12 version 1613; http://www.neuro.uni-jena.de/cat/), which is an add-on of the free Statistical Parametric Mapping (SPM12) software. Briefly, CAT12 integrates a preprocessing step with intensity normalization, bias field inhomogeneity correction, and noise filtering with the SANLMs (spatially adaptive nonlocal means), followed by a registration to a reference template (IXI Dataset; http://www.brain-development.org) using affine and nonlinear transformations. Then, the image is segmented with the help of Markov random field and an adaptive maximum a posteriori method, which reduces the dependency on tissue probability maps.

Second, to assess subcortical structures, the state-of-the-art quality segmentation of the online platform VolBrain software was used (https://www.volbrain.upv.es). A preprocessing step is also performed with intensity normalization, robust bias field inhomogeneity correction with N4 method,[29] denoising with SANLM filter,[30] and finally an affine registration to the MNI space. The segmentation uses the trimmed mean segmentation algorithm combined with a multitemplate method that considers nonlocal label fusion schemes using a library built from the manual segmentation of 50 subjects.[31]

The MP2RAGE image was skull-stripped by using the mask generated by the skull-stripping of the TI2 images obtained with CAT12 before entering the CAT12 and Volbrain pipelines, as already explained by Fujimoto et al.[32]

Contrast ratios (CRs) between structures were calculated using the same equations as in Mussard et al[20] and Okubo et al.[33] To do so, the corresponding masks taken from CAT12 segmentation were used. Contrarily to the conventional contrast-to-noise ratio, CR does not consider the noise of the image to limit possible modifications due to regularization during the CS reconstructions.

Finally, the masks of each brain tissue and structure determined by the 2 different segmentation softwares were applied on the corresponding T_1 maps, to obtain T_1 values from the multiple brain regions studied here.

The mean T_1 of a structure was measured as the average of the T_1 values of each voxel within the structure of interest. Similarly, on the phantom T_1 maps, the mean T_1 values were measured as the mean of the values of each voxel within a region of interest placed on each tube. The T_1 differences were expressed as the difference in T_1 between the reference method (either the fully MP2RAGE or the GRAPPA3-MP2RAGE) and the CS8-MP2RAGE sequence, normalized by the reference method and is expressed in percentage.

To evaluate the segmentation based on the MP2RAGE images with respect to the one obtained from the MPRAGE images, the DICE coefficient, Bland-Altman plots, and the coefficient of variation were used.

- The DICE coefficient measures the overlap between segmented structures obtained from the MPRAGE and the MP2RAGE images. A value of 1 represents a perfect overlap.
- Bland-Altman plots were built considering all subjects and all scan-rescans as the difference between the volumes of each brain structure obtained from the MP2RAGE images and the ones obtained from the MPRAGE images and normalized against the volumes obtained from the MPRAGE images. The lines represent the mean volume difference. The dotted lines represent the 95% limits of agreement, calculated as the mean ± 1.96 × SD (standard deviation).
- Intrapatient repeatability was quantified by the coefficient of variance (CV) among the 3 or 4 values (CV = SD/mean × 100) obtained from each sequence. The CVs were also calculated considering all the participants, so taking the mean and SD of the 51 values (13 participants scanned 3 to 4 times each) obtained from each sequence.

Statistics

Paired Student t tests were performed to compare the volumes segmented from the MPRAGE and the MP2RAGE images for each brain structure. These comparisons were either performed on:

- The 51 values (13 participants scanned 3 to 4 times each) obtained by the MP2RAGE or the MPRAGE analyses (referred to as the whole population thereafter).
- The 3 or 4 values obtained by the MP2RAGE or the MPRAGE analyses at the 3 or 4 scanning sessions of 1 participant. This test was performed for each participant. $P < 0.05$ was considered significantly different.

RESULTS

The CS8-MP2RAGE was acquired in parallel with the standard morphological MPRAGE sequence (Fig. 1) with the same spatial resolution and acquisition time.

As already demonstrated, greater contrasts were obtained on the MP2RAGE images, especially between the GM and the CSF. Indeed, CRs between GM and CSF were 2.17 ± 0.52 and 0.74 ± 0.06 on the MP2RAGE and the MPRAGE images, respectively. In addition, CRs between GM and WM were 0.38 ± 0.01 and 0.15 ± 0.01 on the MP2RAGE and the MPRAGE images, respectively.

As expected, the MP2RAGE image enabled to depict multiple structures in the brain, such as the putamen, the caudate, and the thalamus. These deep gray nuclei were also distinguishable on the MPRAGE image but with lower contrasts, especially the thalamus. Using conventional MP2RAGE parameters, the globus pallidus (or pallidum) was clearly distinguishable on the coronal view of the MP2RAGE images. On the contrary, this structure remains hardly detectable on the MPRAGE images.

The high CS factor may slightly increase the smoothness of the images compared with the parallel imaging acceleration in the MPRAGE

© 2022 The Author(s). Published by Wolters Kluwer Health, Inc.

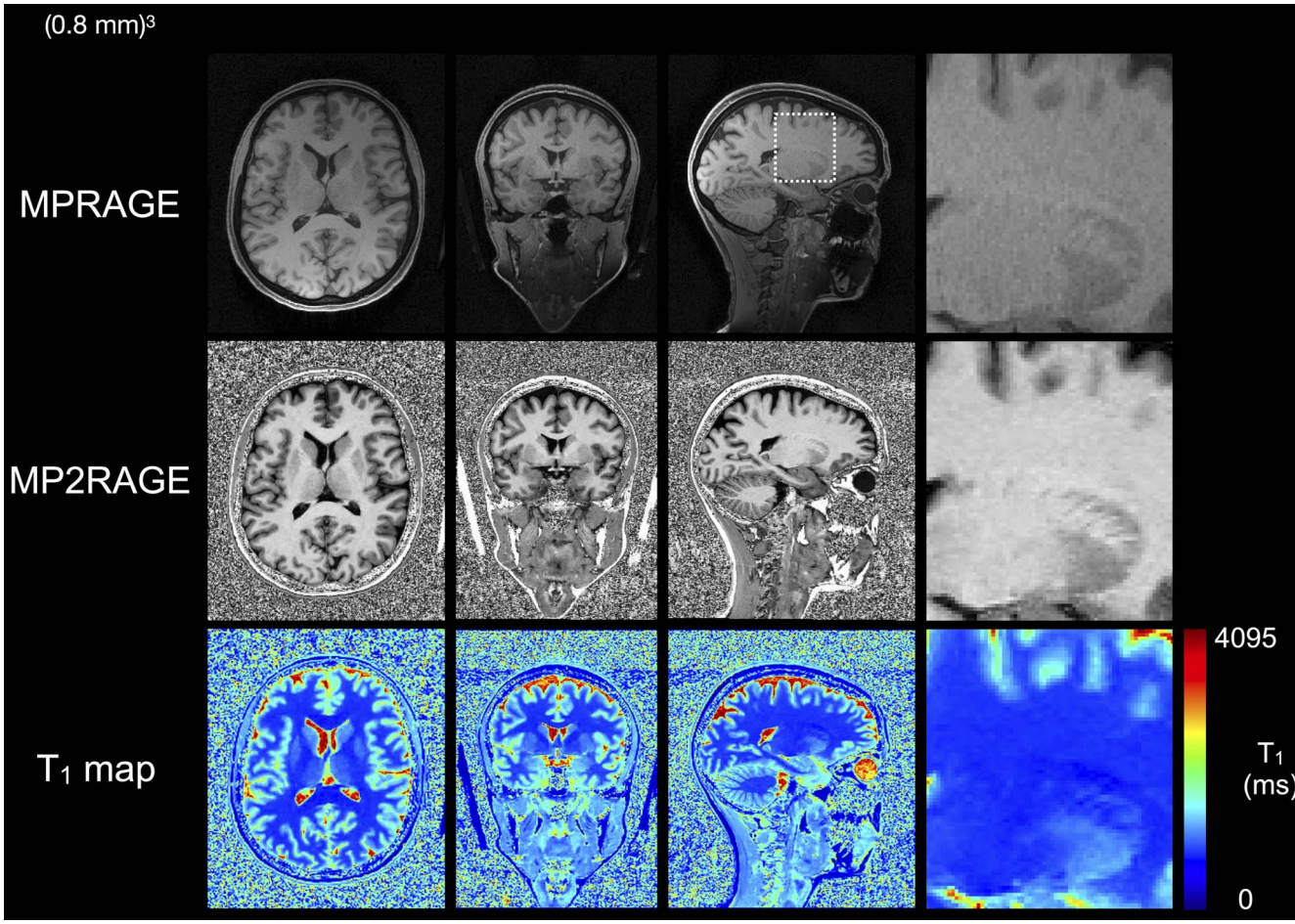

FIGURE 1. Representative MPRAGE and MP2RAGE images of a participant. The T_1 map built from the MP2RAGE images is also shown. The inserts show the striatum (including the putamen and the caudate) to highlight the spatial resolution that is largely preserved on the compressed sensing images.

sequence, but, looking at a fine structure such as the cerebellum, the multiple folia and the WM/GM edges are still very well defined. Also the caudolenticular gray bridges connecting the putamen and the caudate can be depicted and numbered.

In addition to the morphological image, a 3D T_1 map could be generated from the MP2RAGE images, covering the whole brain, with the same high spatial resolution and with a very low noise level.

Large-Scale Morphological Assessment and Volume Repeatability

After the automatic segmentation using the CAT12 software, the mean volumes of WM, GM, and CSF on the 13 participants, each scanned 3 or 4 times at different days of interval, were 713 ± 54, 568 ± 62, and 275 ± 44 cm^3 using the MPRAGE images and 713 ± 53, 572 ± 58, and 268 ± 36 cm^3 using the CS8-MP2RAGE images (Table 1). Consequently, no significant difference across the whole population was observed between the 2 sequences: less than 1% difference was measured ($P = 0.99$ and $P = 0.86$ for GM and WM, respectively), whereas the CSF showed a 2.5% difference, but remained insignificantly different across the whole population scanned in this study ($P = 0.66$).

The intraparticipant differences between the CS8-MP2RAGE and the standard MPRAGE for cerebral tissues were observed more closely with Bland-Altman plots including all the participants and their multiple scan-rescan examinations (Fig. 2). Taking the participants individually, the GM volumes measured from the MP2RAGE images were similar with the ones obtained from the MPRAGE images, except for 3 participants. Even for those, the differences remained less than 5%. The WM volumes measured from the MP2RAGE images were significantly larger than the ones obtained from the MPRAGE images, except for 3 participants whose volumes were similar between the 2 sets of images. However, the WM volume differences were all less than 4% at each session. Finally, the differences in CSF volumes between the MPRAGE and MP2RAGE segmentations show a high variability, ranging from −20% to 12%. Mean intraparticipant segmentation differences of 0.01%, 0.8%, and 1.9% were measured for GM, WM, and CSF, respectively.

In addition, the mean DICE indexes of GM, WM, and CSF were 0.843 ± 0.014, 0.926 ± 0.006, and 0.794 ± 0.041, respectively. To deeply analyze where the differences came from, overlays of the MPRAGE/MP2RAGE images are shown in Figure 3. As expected from the DICE indexes, the WM segmentation was similar between both sequences. The GM segmentation from the MP2RAGE images better delineates inner structures (like the thalamus and the putamen pointed by the blue and white arrows, respectively, in Fig. 3), which could be partly missed by the segmentation from the MPRAGE images. Also, the segmentation from the MP2RAGE images includes more tissue, especially in the cerebellum, than the segmentation extracted from the MPRAGE images. The additional CSF segmented from the MPRAGE images is mainly located around the brain, between the GM and the subarachnoid space, and also in the occipital lobe.

Despite these differences, the intraparticipant variabilities (Fig. 4) in GM, WM, and CSF volumes obtained from the MP2RAGE images

© 2022 The Author(s). Published by Wolters Kluwer Health, Inc.

TABLE 1. GM, WM, and CSF Volumes Measured From the MP2RAGE or the MPRAGE Segmentations Using SPM for Each Individual

Individual Number	Sequence	GM, cm^3	WM, cm^3	CSF, cm^3
Ind_1	MPRAGE	743.6 ± 4.3	537.2 ± 2.6	289.6 ± 4.2
	MP2RAGE	735 ± 7.3	543.2 ± 3.5	268.3 ± 3.9*
Ind_2	MPRAGE	682.5 ± 3	591.9 ± 5	292.1 ± 7.4
	MP2RAGE	685.6 ± 16.2	593.2 ± 2	276.9 ± 14.8
Ind_3	MPRAGE	647.4 ± 4.2	493.7 ± 1.1	247 ± 3.7
	MP2RAGE	650.8 ± 3.6	498.2 ± 1.5*	241.4 ± 3
Ind_4	MPRAGE	700.7 ± 5.3	490.6 ± 4.8	259.6 ± 11.7
	MP2RAGE	692.5 ± 8.4	504.6 ± 1.5*	234.3 ± 10.2*
Ind_5	MPRAGE	708.8 ± 5.8	642.4 ± 1.1	292.5 ± 5.8
	MP2RAGE	711.3 ± 6.7	642.4 ± 2.6	293.1 ± 8
Ind_6	MPRAGE	794 ± 3.6	641 ± 2.4	370.1 ± 2.3
	MP2RAGE	813.5 ± 4.4*	651 ± 2.2*	361 ± 2*
Ind_7	MPRAGE	762.7 ± 1.3	624.2 ± 1.9	285.5 ± 1.5
	MP2RAGE	769.7 ± 1.3*	627.2 ± 1*	267.4 ± 2.2*
Ind_8	MPRAGE	692 ± 1.6	543.7 ± 1.1	243.8 ± 1.6
	MP2RAGE	690.4 ± 1.8	550.8 ± 3*	255.8 ± 3*
Ind_9	MPRAGE	653.7 ± 3.6	486 ± 1.1	211.9 ± 4.2
	MP2RAGE	652.8 ± 3.6	488.9 ± 1.2*	215.5 ± 2.5
Ind_10	MPRAGE	685.9 ± 5	556.2 ± 2.1	283.8 ± 5.6
	MP2RAGE	695.2 ± 6.8	561 ± 1.2*	279.1 ± 8.9
Ind_11	MPRAGE	810 ± 4.9	672.6 ± 2	208 ± 3.9
	MP2RAGE	781.7 ± 7*	653.1 ± 3.7*	242.1 ± 11.7*
Ind_12	MPRAGE	746 ± 4	544.1 ± 1.7	322.2 ± 1.2
	MP2RAGE	749 ± 3	557.8 ± 2.1*	286.5 ± 3.8*
Ind_13	MPRAGE	646.6 ± 3.7	559 ± 1	265.9 ± 2.1
	MP2RAGE	644.5 ± 7.8	566 ± 3.6*	261.2 ± 2.7*

The asterisks indicate a significant difference of volume between the MPRAGE and the MP2RAGE sequences.

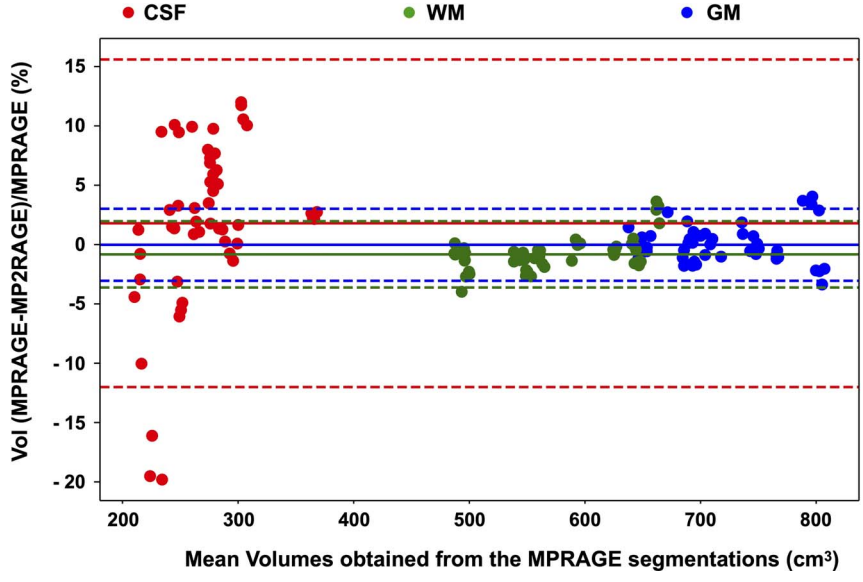

FIGURE 2. Bland-Altman plot showing the volume differences of WM (green dots), GM (blue dots), and CSF (red dots) between the MPRAGE and the MP2RAGE segmentations. The lines show the mean volume difference, and the dotted lines show the 95% confidence interval.

© 2022 The Author(s). Published by Wolters Kluwer Health, Inc.

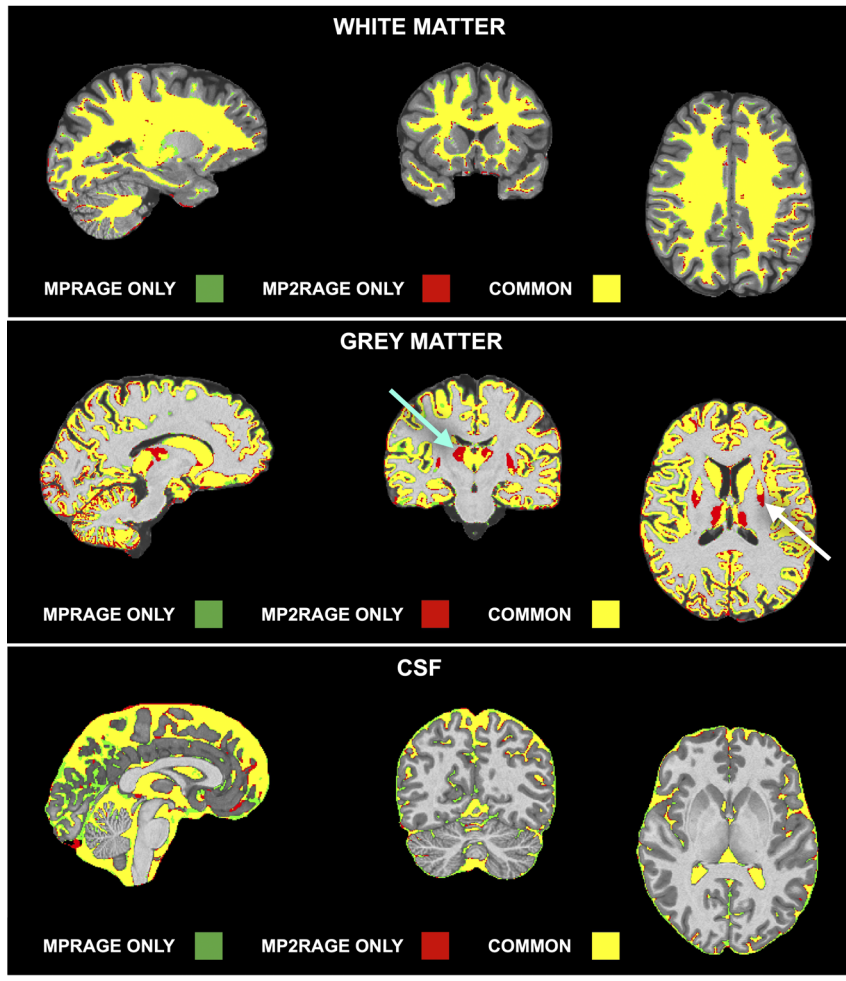

FIGURE 3. Representative overlays between MP2RAGE and MPRAGE segmentations of WM, GM, and CSF in 1 participant. The white arrow and the blue arrow point at the putamen and the thalamus, respectively, within which some areas are included into the GM segmentation with the MP2RAGE images but not with the MPRAGE images.

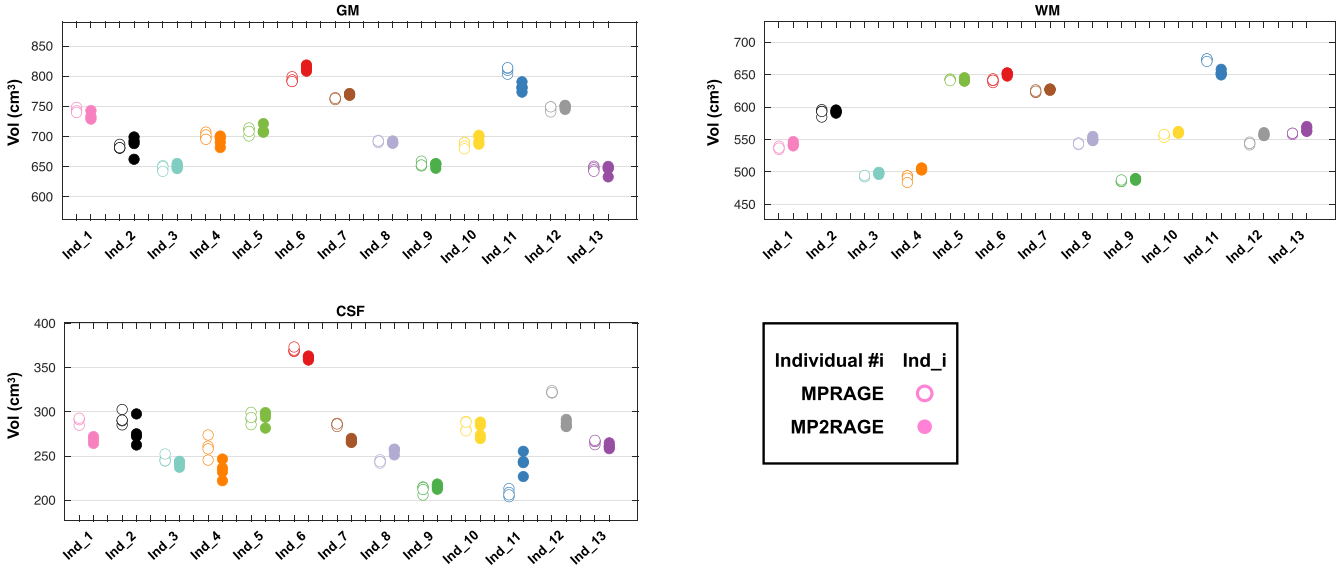

FIGURE 4. WM, GM, and CSF volumes segmented from the MPRAGE (circles) or MP2RAGE (dots) images, for each individual (noted Ind_i and represented by different colors).

© 2022 The Author(s). Published by Wolters Kluwer Health, Inc.

were low: less than 2.4%, 0.7%, and 5.4% for GM, WM, and CSF, respectively. Similarly, these variabilities using the MPRAGE images were less than 1% for GM and WM and 4.5% for CSF.

Subcortical Structures Volume Evaluation and Repeatability

One of the advantages of the MP2RAGE over the MPRAGE images are the higher contrasts between brain structures, at high magnetic fields. We thus intended to segment the deep gray nuclei using the segmentation software VolBrain.

The volumes measured on the 13 participants, each scanned 3 or 4 times, were compared after their segmentations obtained from the MPRAGE or the MP2RAGE images. For the intracerebral structures studied here, the Bland-Altman plot demonstrates a good similarity in the volume measurements between the MPRAGE and the MP2RAGE sequences, especially for structures larger than 4 cm^3 (Fig. 5). More precisely, similar volumes (less than 4.1% difference) between MP2RAGE and MPRAGE segmentations were obtained for the putamen. Of note, 1 participant harbors a large putamen (approximately 12.5 cm^3), but the segmentations from the MPRAGE and the MP2RAGE images are quasi-identical (less than 1% difference). The mean caudate and hippocampus volumes measured from the MP2RAGE images were significantly smaller than the ones obtained from the MPRAGE images, of maximum 6.4% and 8.5%, respectively. On the contrary, the thalamus volumes measured from the MP2RAGE images were significantly larger than the ones obtained from the MPRAGE images; yet, the volumes were less than 8.2% different for all the participants, except for 1 (Ind_4) whose mean difference reached 24.7% in 1 session, due to a failure of the MPRAGE segmentation (encircled green dot and also visible in Fig. 6). For smaller structures (volume less than 4 cm^3) such as the accumbens, amygdala, and pallidum, these differences between the MPRAGE and the MP2RAGE segmentations could reach −25% to 13.5%. Taking the participants as a whole population, the mean pallidum volumes were 6.5% larger on the MP2RAGE images than on the MPRAGE images, similarly as for the accumbens, whose mean volumes were 2.8% larger. Nevertheless, the mean amygdala volumes were identical between the 2 sets of images.

The DICE indexes between the MPRAGE and the MP2RAGE segmentations of the subcortical structures were high; 0.93 for the thalamus, the caudate, the putamen, and the hippocampus structures. Nevertheless, this index decreased to 0.88 for the amygdala and the globus pallidus, and reached 0.83 for the accumbens. Representative overlays of the 2 segmentations are shown in Figure 6 and demonstrate that the differences mainly come from structure boundaries (arrow in Fig. 6).

The intraparticipant volume variabilities obtained from the MP2RAGE images acquired on the 13 volunteers were extremely low (Fig. 7): less than 3% for the hippocampus, caudate, putamen, and thalamus. Similar variabilities were obtained using the MPRAGE segmentation for the large structures. For the smaller structures, the variabilities obtained from the MP2RAGE segmentations were less than 3.7% for the globus pallidus (except 6.4% variability for Ind_1), less than 8% for the amygdala, and less than 6.3% for the accumbens. In parallel, the MPRAGE segmentations showed variabilities of less than 3% for the globus pallidus (except for Ind_4 which has a 6.6% variability), less than 4.8% for the amygdala, and less than 4.7% for the accumbens.

Considering all the participants as a whole population, the coefficients of variance of the segmentations from the MPRAGE or the MP2RAGE images were as follows: 3.9% or 2.8% for accumbens, respectively; 0.6% or 0.4% for caudate, respectively; 2.1% or 2% for pallidum, respectively; 4.2% or 2.4% for amygdala, respectively; and 0.6 or 0.6 for hippocampus, respectively.

Assessment and Repeatability of T_1 Measurements

T_1 measurements were performed on a phantom using the CS8-MP2RAGE and the constructor MP2RAGE sequence either fully sampled or accelerated with GRAPPA3 (Table 2). Less than 5% difference was found between the measurements obtained with the fully MP2RAGE and the CS8-MP2RAGE, and also between the GRAPPA3-MP2RAGE and the CS8-MP2RAGE. Also, small standard deviations were obtained, highlighting high accuracy in the T_1 measurements for all the sequences.

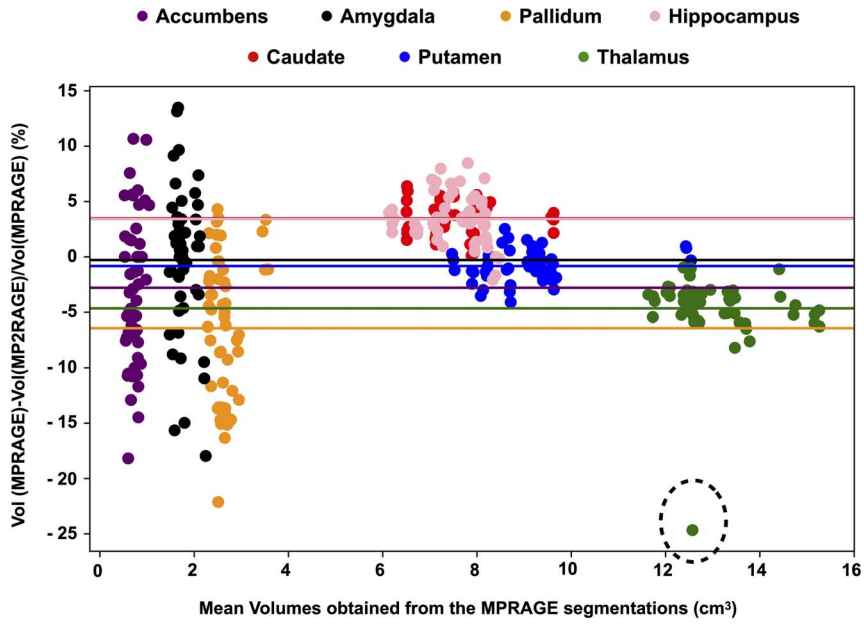

FIGURE 5. Bland-Altman plot showing the volume differences of the deep gray nuclei studied here (thalamus [green dots], putamen [blue dots], caudate [red dots], hippocampus [pink dots], pallidum [orange dots], amygdala [black dots], accumbens [purple dots]), between the MPRAGE and the MP2RAGE segmentations. The dotted circle shows the large discrepancy between the 2 segmentations of the thalamus, which occurred in 1 patient at 1 scan session.

© 2022 The Author(s). Published by Wolters Kluwer Health, Inc.

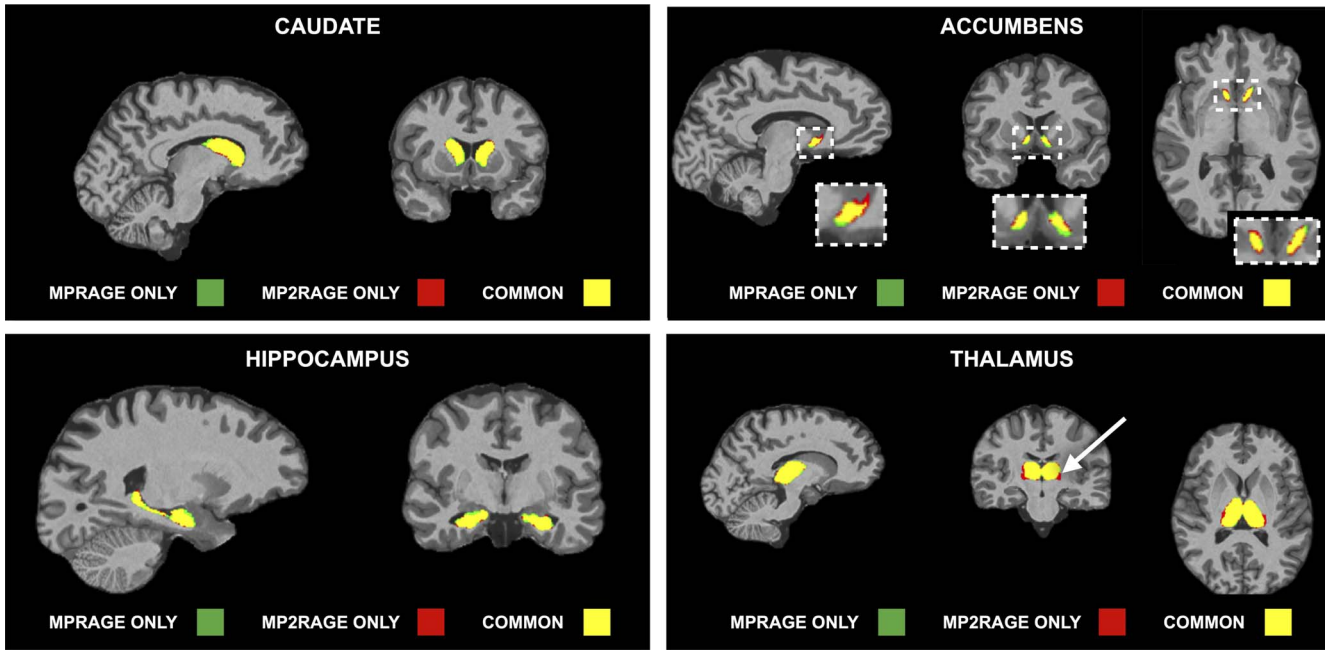

FIGURE 6. Representative overlays between MP2RAGE and MPRAGE segmentations of several deep gray nuclei: caudate and hippocampus, for which the segmented volumes are smaller from the MP2RAGE images than from the MPRAGE images; thalamus, for which the segmented volumes are larger from the MP2RAGE images than the MPRAGE images. The white arrow points at the larger segmentations obtained from the MP2RAGE images.

On the volunteers, the T_1 values of the WM and GM were in the range of the ones found in the literature, but with a trend to be slightly longer than previously reported values measured with the MP2RAGE sequence (Table 3). More specifically, the WM and GM T_1 values obtained with the sequence developed in the current study were 5.2% and 6.3% longer than the ones obtained with the CS-MP2RAGE from Mussard et al[20]; also, these values were 5.6% and 4% longer than the ones obtained with the GRAPPA3-MP2RAGE sequence. Among all the MP2RAGE sequences shown in Table 3, the current values are thus the closest to the standard inversion-recovery sequences (less than 3% difference between the 2 sequences). Still, as expected, the WM T_1 values obtained with the current MP2RAGE

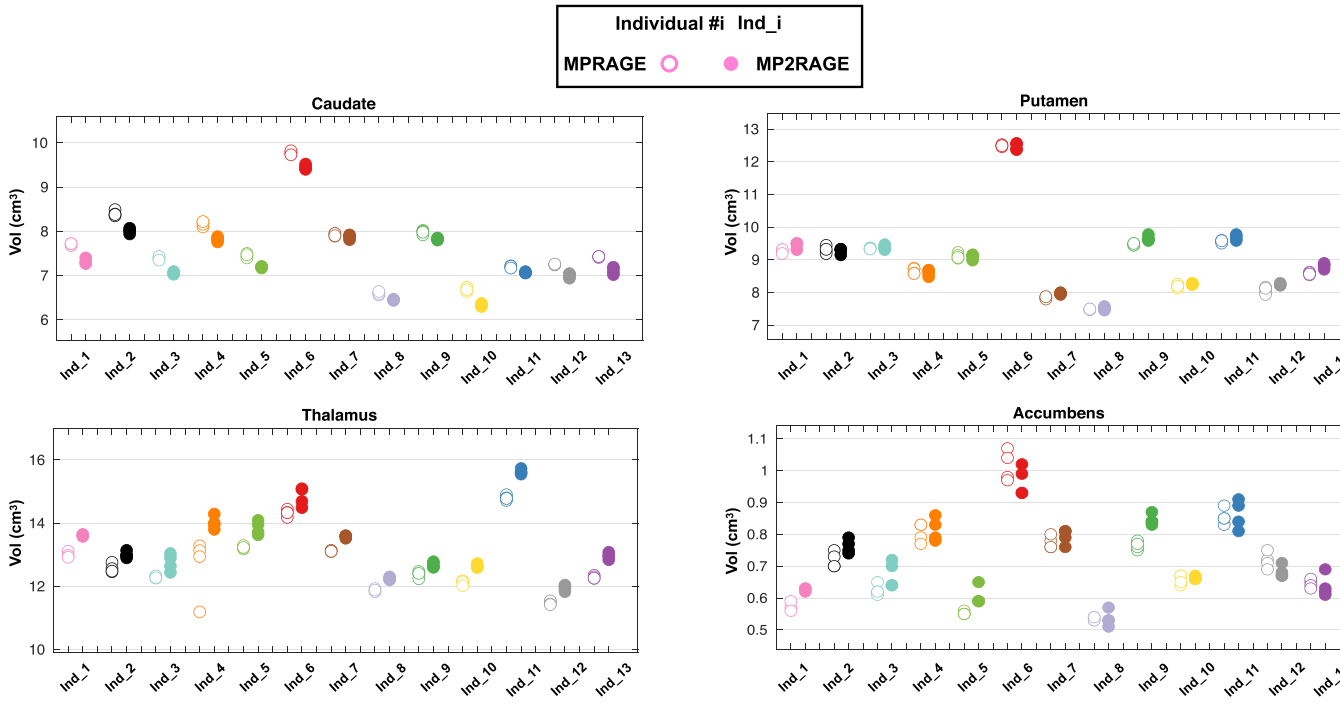

FIGURE 7. Volumes of the some deep gray nuclei (caudate, thalamus, putamen, and accumbens) segmented from the MPRAGE (circles) or MP2RAGE (dots) images, for each individual (noted Ind_i and represented by different colors).

© 2022 The Author(s). Published by Wolters Kluwer Health, Inc.

TABLE 2. T1 Values of Phantoms Obtained With the CS8-MP2RAGE Sequence and the Corresponding Differences With the Reference Constructor MP_2RAGE Sequences (Either Fully Sampled or GRAPPA3-Accelerated)

Gd-DOTA Concentrations, mM	Sequence	Phantom 1 T_1, ms	Phantom 2 T_1, ms	Phantom 3 T_1, ms	Mean Error With Fully MP2RAGE, %	Mean Error With GRAPPA3-MP2RAGE, %
0	CS8-MP2RAGE	2333.9 ± 47	2515.1 ± 85.4	2338.7 ± 55.5	−0, 140389519	1, 687208737
	MP2RAGE fully	2362.8 ± 48.2	2411.6 ± 77.6	2402.3 ± 78.7		
	GRAPPA3-MP2RAGE	2367.5 ± 87.7	2505.2 ± 111.9	2437.1 ± 103		
0.01	CS8-MP2RAGE	2201.4 ± 59.7	2167.3 ± 68.4	2051.1 ± 36.1	2, 774512501	4, 056894356
	MP2RAGE fully	2192.7 ± 71.6	2251.1 ± 50.3	2159 ± 41.8		
	GRAPPA3-MP2RAGE	2219.7 ± 109	2302.7 ± 71.8	2169.7 ± 66.9		
0.02	CS8-MP2RAGE	1942 ± 47.9	1862.8 ± 56.5	1850.9 ± 45.4	2, 940030928	3, 40914555
	MP2RAGE fully	1943.9 ± 47.1	1981 ± 56.8	1903.4 ± 41.6		
	GRAPPA3-MP2RAGE	1953.2 ± 75.8	1986.8 ± 75.5	1916.3 ± 70		
0.04	CS8-MP2RAGE	1734.5 ± 37.3	1670.8 ± 43.1	1574.9 ± 26.9	1, 601465069	1, 777329097
	MP2RAGE fully	1743.1 ± 50.2	1738.15 ± 48	1581.8 ± 36.3		
	GRAPPA3-MP2RAGE	1739 ± 60.1	1739.5 ± 55.8	1592.8 ± 46.9		
0.05	CS8-MP2RAGE	1482.4 ± 26.6	1460.9 ± 40.9	1406.8 ± 33.6	2, 33602128	2, 545889973
	MP2RAGE fully	1498.7 ± 26.9	1514.2 ± 32.7	1441.4 ± 37.6		
	GRAPPA3-MP2RAGE	1500.1 ± 37.2	1520.9 ± 49.8	1443.1 ± 51.4		
0.15	CS8-MP2RAGE	953.7 ± 13.9	945.7 ± 19.1	946.1 ± 19.5	2, 517743661	2, 314453792
	MP2RAGE fully	973.8 ± 16.3	975 ± 19.7	970.2 ± 18.9		
	GRAPPA3-MP2RAGE	966.2 ± 20.6	975.1 ± 21.3	971.7 ± 20.8		
0.2	CS8-MP2RAGE	695.3 ± 8.9	659.5 ± 12.5	600.8 ± 11.6	2, 731082091	1, 775987874
	MP2RAGE fully	712.3 ± 13.8	681 ± 11.1	617.1 ± 10.1		
	GRAPPA3-MP2RAGE	702.8 ± 12.1	677.1 ± 13.8	610.9 ± 12.6		
0.3	CS8-MP2RAGE	499.3 ± 9.2	500.7 ± 15	469.4 ± 10.7	2, 925134787	1, 829614104
	MP2RAGE fully	513.9 ± 9.9	514.9 ± 8.2	484.8 ± 10.5		
	GRAPPA3-MP2RAGE	505.3 ± 12.2	510.5 ± 14.2	480.9 ± 11.8		

TABLE 3. T_1 Values (in milliseconds) of Multiple Brain Structures Obtained From Our Study and the Corresponding Literature

	Sequence Used	WM	GM	Caudate	Putamen	Thalamus	Globus Pallidus	Hippocampus
From the current study	CS8-MP2RAGE	857.4 ± 25.9	1416.8 ± 20.8	1274.7 ± 10.3	1135 ± 7.3	1034.1 ± 6.3	899.8 ± 7.2	1338.1 ± 17.7
From Marques et al[14]	GRAPPA-MP2RAGE	810 ± 30	1390 ± 70	1250 ± 70	1130 ± 70	1080 ± 70	970 ± 70	
From Mussard et al[20]	GRAPPA-MP2RAGE	829.8 ± 13	1338.4 ± 20.7	1219.6 ± 13.9	1127.1 ± 8.3	1035.5 ± 5.5		1377.3 ± 40.9
From Mussard et al[20]	CS4-MP2RAGE	820.3 ± 14.9	1332.4 ± 30.7	1188.5 ± 14.7	1098.9 ± 14.3	1012.2 ± 11.3		1340.9 ± 54.5
From Okubo et al[33]	GRAPPA-MP2RAGE			1217 ± 30	1095 ± 31	1077 ± 30	877 ± 18	
From Rioux et al[34]	IR	882 ± 19						
From Rioux et al[34]	IR + biexp fit	939 ± 14						
From Dieringer et al[35]	VFA	969 ± 85	1433 ± 80					
From Dieringer et al[35]	IR	911 ± 15	1615 ± 149					
From Dezortova et al[36]	IR			1342.8 ± 32.6	1210.6 ± 43.8	1140.4 ± 38.4	1028.4 ± 43.7	
From Jutras et al[37]	MP2R1	810 ± 17		1344 ± 20	1209 ± 30		924 ± 36	
From Jutras et al[37]	VFA	851 ± 50		1391 ± 51	1225 ± 36		968 ± 39	
From Preibisch and Deichmann[38]	VFA	933 ± 15	1380 ± 59	1450	1310			
From Preibisch and Deichmann[38]	IR-EPI	894 ± 23						
From Oros-Peusquens et al[39]	TAPIR			1226 ± 53	1140 ± 41	1016 ± 40	888 ± 31	
From Gelman et al[40]	Look-Locker	844		1481	1335	1217	1041	
From Wansapura et al[41]	SatRec-VariableTR-SE	832	1331					
From Weiskopf et al[42]	MPM	965	1642	1464				

© 2022 The Author(s). Published by Wolters Kluwer Health, Inc.

sequence were approximately 6.5% shorter than the criterion standard IR sequences.[34,35]

The T_1 of CSF was calculated to be 2609 ± 141 milliseconds. All the volunteers had CSF T_1 values longer than 2424 milliseconds, whereas 1 volunteer had T_1 of 2260 ± 27 milliseconds.

The intraparticipant T_1 variabilities were less than 2.7%, 1.2%, and 0.7% for CSF, GM, and WM, respectively. The corresponding variabilities when the 13 volunteers are considered as a whole population were 5.4%, 1.5%, and 2.1% for CSF, GM, and WM, respectively.

The T_1 values of the subcortical structures (Fig. 8A) were also compared with the literature (Table 3). In general, the estimated T_1 values were consistent with the literature. Also, due to the high accuracy of the measurements, the T_1 of the 3 substructures of the hippocampus (CA1-3, CA4-DG, and subiculum) could be distinguished (Fig. 8B).

The T_1 variability within the subcortical structures over the scan-rescans was excellent (Fig. 8A). It was less than 2% for all the subcortical structures, although for the accumbens, the variability could reach 2.8%.

DISCUSSION

Here, we developed and optimized both the acquisition and reconstruction of a CS-accelerated MP2RAGE sequence to provide a protocol of less than 10 minutes. During the 3 minutes 33 seconds of reconstruction time, subsequent acquisitions can be performed without perturbing the clinical examination. Consequently, this protocol meets the requirements for clinical procedures. The performance of this protocol in terms of brain structure segmentation and volume estimation has been investigated and compared with the conventional MPRAGE method currently used routinely in clinical research protocols. Replacing the MPRAGE sequence with the highly accelerated MP2RAGE sequence would have the advantage of additionally providing T_1 maps, a quantitative measure that gives informative insights on tissue microstructure.

To reach the same acquisition time with the MP2RAGE and the MPRAGE sequences, a CS-accelerated MP2RAGE was developed and tested. This study was conducted using a 0.8-mm isotropic resolution to answer to the increasing demand of higher spatial resolution to better characterize deep brain structures. Nevertheless, such increase of the resolution alters the SNR of the images, which could in turn affect the sensitivity and precision of both the volumes and the T_1 measurements. To assess this, we chose to use widely-used segmentation tools that are already used for analyzing MPRAGE images, in the perspective of using the MP2RAGE sequence without any additional software to purchase and to not generate any bias in the analyzes. This implies that the

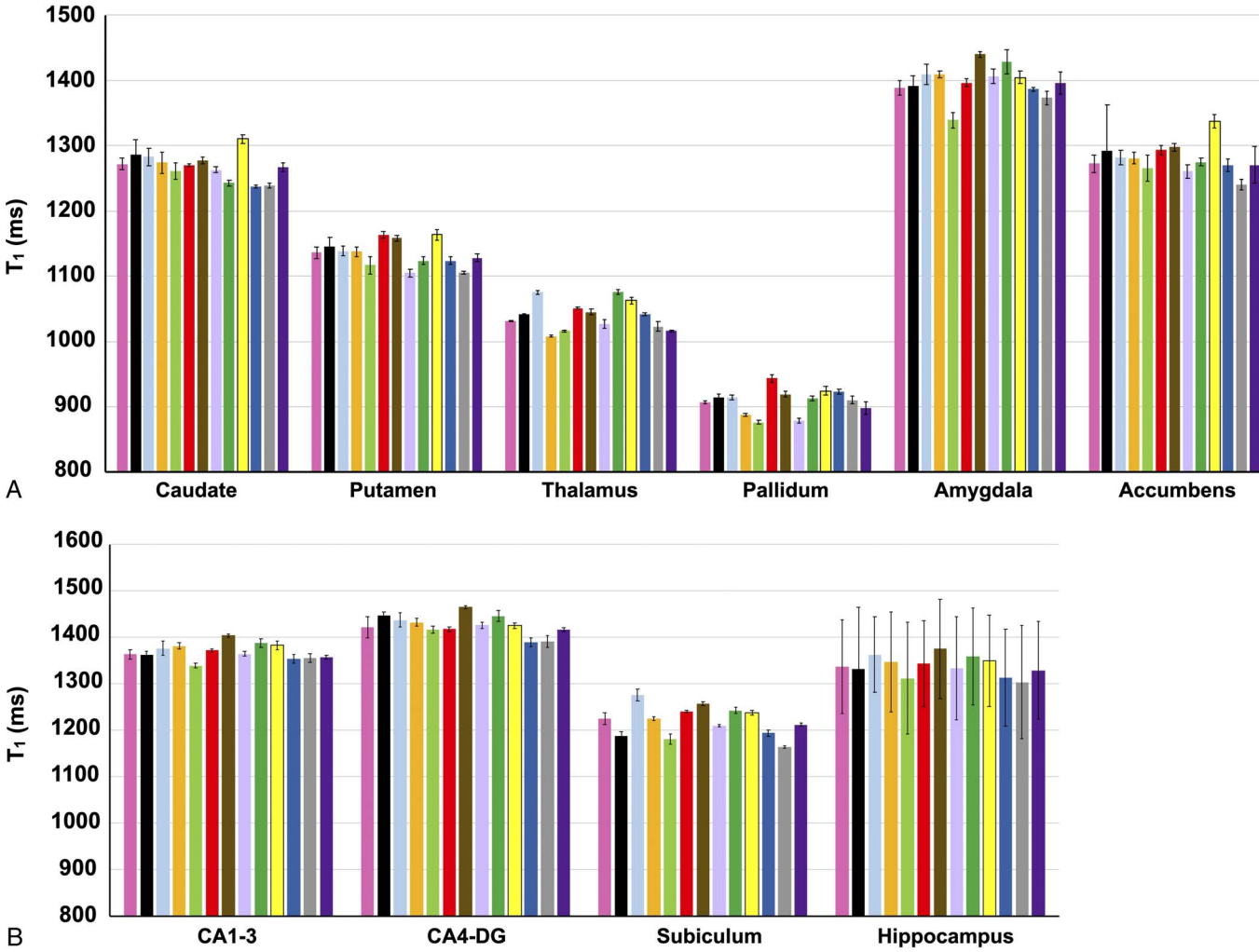

FIGURE 8. Mean T_1 values calculated over the multiple scan sessions in each individual of the deep gray nuclei studied here (A) and also of the substructures of the hippocampus (B). The colors represent each individual. The error bars are the standard deviations across the 3 or 4 scans in one given participant.

© 2022 The Author(s). Published by Wolters Kluwer Health, Inc.

softwares are actually based on MPRAGE contrasts, and consequently, the segmentation from the MP2RAGE images could be improved by using a dedicated software, such as MorphoBox (a Siemens Healthcare prototype). Another important parameter of comparison that our study assessed is the scan-rescan reproducibility of independent examinations, that is, on participants scanned 4 times minimum and at several days of interval; this could represent the serial follow-up of patients during their care. This type of repeatability has not been evaluated previously.

Our study is the first one to evaluate volume differences of brain structures between the CS-accelerated MP2RAGE and the standard morphological MPRAGE. Indeed, Mussard et al[20] only compared the CS-MP2RAGE and the parallel imaging accelerated MP2RAGE. Here, volumetric measurements demonstrated that the MP2RAGE sequence can perform as well as the MPRAGE sequence. Also, the WM and GM volumes obtained from the MP2RAGE images are in accordance with previous studies.[43] Previously, volume differences between the MPRAGE and the GRAPPA-accelerated MP2RAGE segmentations have already been measured using different softwares; CAT12, VolBrain, FSL-FAST, SIENA/X, SPM, FIRST, and MorphoBox.[44–46] In these latter studies, although a nonconcordance of the acquisition parameters between the 2 sequences lead to differences in acquisition time and/or spatial resolution, the authors highlight the high repeatability of the segmentation results for both sequences. Here, a comparison between the MPRAGE and the CS-accelerated MP2RAGE sequences acquired with the same resolution and acquisition time was performed. This enabled to highlight that (1) by using CAT12 on the MPRAGE images, some parts of some deep gray nuclei are misregistered into WM tissue due to the low contrast between GM and WM, and (2) the CSF volume segmented from the MPRAGE images tends to be overestimated. As already mentioned in previous studies, this might be due to the similar signal intensities between the CSF and the skull on the MPRAGE images,[45] compared with the high contrasts between these tissues on the MP2RAGE images. In addition, skull stripping procedures were applied differently: it is performed on the TI2 images not on the MP2RAGE ones due to the salt-and-pepper background noise, whereas it is directly performed on the MPRAGE images. Consequently, this procedure might crop the skull differently between the MPRAGE and MP2RAGE images and then include more voxels in the CSF mask during the MPRAGE segmentation.

For subcortical regions, the software VolBrain was used as it has been shown to lead to the most precise and true values of volumes compared with manual segmentations for the thalamus and hippocampus when using the GRAPPA-accelerated MP2RAGE sequence.[47] The volumes obtained from these manual delineations are in line with the volume estimations obtained here with the current CS8-MP2RAGE. For the other nuclei, their volumes are within the range of the ones found in literature.[43,44] Consequently, even using a nondedicated segmentation tool, the parcellation on the MP2RAGE images could be performed. The high DICE indexes and the Bland-Altman plots suggest that the segmentations with the MP2RAGE and the MPRAGE are equivalent and highly reproducible, especially for large subcortical nuclei. Segmentations of small structures are challenging. Volume differences between the 2 sequences might come from differences in contrasts between the 2 sets of images,[33,44] the nonoptimization of the parameters of the segmentation softwares used, and the small sizes of some nuclei that can be largely affected even for low differences in amount of voxels. For the thalamus specifically, our results are in accordance with Okubo et al,[33] who explains the difference of segmentation between the GRAPPA3-MP2RAGE and the MPRAGE by its very low CR.

Importantly, the variability of the subcortical volumes segmented from the CS-accelerated MP2RAGE images performed in our study is similar as the one measured by Mussard et al,[20] although here, 4 to 5 scan-rescans were performed at several days of interval, compared with a scan-rescan without repositioning.

The CS8-MP2RAGE sequence also provides T_1 maps. A high accuracy in T_1 measurements was obtained compared with the standard MP2RAGE sequences (either fully sampled or accelerated with parallel imaging), although different acquisition parameters and reconstruction methods were used. On the human brain, T_1 values obtained with the accelerated protocol were very similar to the literature and showed high repeatability. As previously reported in the literature, differences between the MP2RAGE and the IR sequence were measured. This difference might come from the magnetization transfer effect.[34] Nevertheless, the T_1 values obtained with the CS8-MP2RAGE method are closer to the ones obtained with the IR sequence compared with other MP2RAGE methods in literature. Differences among the MP2RAGE methods might come from different implementations of RF and gradient spoiling, which would lead to inaccuracies in the T_1 measurements, especially for structures with long relaxation times, such as the CSF.[48] Several advantages make the CS-MP2RAGE more suitable for neuroimaging than the popular DESPOT1 method.[49] Indeed, as this latter sequence uses multiple flip angles, patient motion between the acquisitions can occur and the acquisition of an additional B1+ map for correction is mandatory. Also this method remains long (>8 minutes for a 1-mm isotropic whole-brain T_1 map), although the reconstruction time is fast (less than 1 minute). The MP2RAGE sequence is faster than standard Look-Locker–based T_1 mapping sequences, due to the ETL acceleration. However, recent new reconstruction methods that use the high numbers of inversion points (like model-based or subspace) have the potential to reduce the differences in acquisition times between the 2 sequences.[50,51] Consequently, the CS-MP2RAGE sequence is a convincing tool within the panel of T_1 mapping sequences for the clinical MRI community. Another tremendously important feature is the intersubject variations of T_1, which were extremely low in the current study, and thus may be beneficial for differentiating pathological from healthy tissue. The similar accuracy of the CS8-MP2RAGE with the vendor MP2RAGE sequence ensures a precise longitudinal follow-up of patients.

Given all these results, the MP2RAGE sequence could be considered equivalent to the reference morphological MPRAGE, but with caution, due to differences in CSF volumetric measurements. Nevertheless, due to the very high repeatability of both the volumes and the T_1 values provided by the CS-accelerated MP2RAGE sequence, and the similar WM and GM volumes between the standard MPRAGE and the current MP2RAGE sequences, the latter could be included into a longitudinal protocol. However, we would not recommend to switch from MPRAGE to MP2RAGE sequence in the middle of the scanning of a cohort, unless only T_1 values are taken into account. Instead, we recommend to use the MP2RAGE sequence and associate it with 1 segmentation tool for any new studies given the additional T_1 map, and thus a quantitative biomarker to conduct longitudinal studies, while maintaining the same acquisition time and repeatability.

Limitations

The CS-accelerated MP2RAGE acquisition duration could be further shortened by increasing the amount of echoes per train, like in Mussard et al.[20] In our case, lengthening to 195 echoes per train in the CS8-MP2RAGE acquisition would shorten the duration by 36% but decrease CNR between GM and WM (Suppl Fig. 2, http://links.lww.com/RLI/A667). Also, increasing the echo train length can generate wider point spread function, due to the large signal variation along the magnetization recovery, and consequently would decrease the accuracy of both the segmentations and T_1 measurements.[16] In parallel, the reconstruction time could be further shortened via optimization of the Matlab code, upgrade to more recent release of Gadgetron and BART library, and the use of parallel processing (GPU).

No manual segmentation from a neuroradiologist was performed to limit subjective and time-consuming analyses. Also, the tracing of the deep gray nuclei can be unreliable due to the low CR at their boundaries. To only base our conclusions on widely open-access segmentation softwares and because many works have studied the MPRAGE

© 2022 The Author(s). Published by Wolters Kluwer Health, Inc.

segmentation, the automatic segmentation of the MPRAGE images was considered as a "silver standard" in our study.

Availability of the CS-MP2RAGE sequence and reconstruction on a clinical scanner is yet not possible in clinical routine. That is why the CS-MP2RAGE sequence developed here can be provided upon request. We also share the open-source code of the reconstruction through Gadgetron making validation and reproducibility of the results easier. In this study, not only the acquisition duration was improved, but the reconstruction time was also minimized. Indeed, these criteria are critical in the perspective of transferring an innovative method in clinical routine. This information was not mentioned in the previous article using the CS-MP2RAGE on humans. In our study, the rapidity of the pipeline developed here can further benefit from the actively pursuing developments of the users of the Gadgetron. Also, the advantage of this software is that new processing can be easily added into the pipeline to send more information to the user, such as the undersampled images.

The setup of the sequence and the reconstruction is only available on Siemens systems. Stikov and Karakuzu are currently starting an initiative to implement a vendor agnostic acquisition and reconstruction T_1 map based on a variable flip angle sequence and show great promise.[52,53] It can be extended to other MR sequences such as the CS-MP2RAGE. This strategy might increase the impact of quantitative MRI for longitudinal follow-up by reducing variabilities.

Conclusions

In conclusion, the CS-MP2RAGE sequence provides morphological images with similar quality as the standard MPRAGE sequence. Consequently, it can be considered as an alternative to the MPRAGE sequence when additional T_1 maps are necessary. The high repeatability in brain structure volumes and T_1 measurements can be of tremendous interest in longitudinal studies of the human brain.

REFERENCES

1. deSouza NM, Achten E, Alberich-Bayarri A, et al. Validated imaging biomarkers as decision-making tools in clinical trials and routine practice: current status and recommendations from the EIBALL* subcommittee of the European Society of Radiology (ESR). *Insights Imaging*. 2019;10:87.
2. Hagiwara A, Fujita S, Ohno Y, et al. Variability and standardization of quantitative imaging: monoparametric to multiparametric quantification, radiomics, and artificial intelligence. *Invest Radiol*. 2020;55:601–616.
3. Callaghan MF, Freund P, Draganski B, et al. Widespread age-related differences in the human brain microstructure revealed by quantitative magnetic resonance imaging. *Neurobiol Aging*. 2014;35:1862–1872.
4. Kupeli A, Kocak M, Goktepeli M, et al. Role of T1 mapping to evaluate brain aging in a healthy population. *Clin Imaging*. 2020;59:56–60.
5. Hagiwara A, Fujimoto K, Kamagata K, et al. Age-related changes in relaxation times, proton density, myelin, and tissue volumes in adult brain analyzed by 2-dimensional quantitative synthetic magnetic resonance imaging. *Invest Radiol*. 2021;56:163–172.
6. Lutti A, Dick F, Sereno MI, et al. Using high-resolution quantitative mapping of R1 as an index of cortical myelination. *Neuroimage*. 2014;93:176–188.
7. Vrenken H, Geurts JJ, Knol DL, et al. Whole-brain T1 mapping in multiple sclerosis: global changes of normal-appearing gray and white matter. *Radiology*. 2006;240:811–820.
8. Blystad I, Håkansson I, Tisell A, et al. Quantitative MRI for analysis of active multiple sclerosis lesions without gadolinium-based contrast agent. *AJNR Am J Neuroradiol*. 2016;37:94–100.
9. Dean DC 3rd, Sojkova J, Hurley S, et al. Alterations of myelin content in Parkinson's disease: a cross-sectional neuroimaging study. *PLoS One*. 2016;11:e0163774.
10. Bernhardt BC, Fadaie F, Vos de Wael R, et al. Preferential susceptibility of limbic cortices to microstructural damage in temporal lobe epilepsy: a quantitative T1 mapping study. *Neuroimage*. 2018;182:294–303.
11. Anzai Y, Ishikawa M, Shaw DW, et al. Paramagnetic effect of supplemental oxygen on CSF hyperintensity on fluid-attenuated inversion recovery MR images. *AJNR Am J Neuroradiol*. 2004;25:274–279.
12. Lescher S, Jurcoane A, Veit A, et al. Quantitative T1 and T2 mapping in recurrent glioblastomas under bevacizumab: earlier detection of tumor progression compared to conventional MRI. *Neuroradiology*. 2015;57:11–20.
13. Nöth U, Tichy J, Tritt S, et al. Quantitative T1 mapping indicates tumor infiltration beyond the enhancing part of glioblastomas. *NMR Biomed*. 2019;33:e4242.
14. Marques JP, Kober T, Krueger G, et al. MP2RAGE, a self bias-field corrected sequence for improved segmentation and T1-mapping at high field. *Neuroimage*. 2010;49:1271–1281.
15. Metere R, Kober T, Möller HE, et al. Simultaneous quantitative MRI mapping of T1, T2* and magnetic susceptibility with multi-echo MP2RAGE. *PLoS One*. 2017;12:e0169265.
16. Caan MWA, Bazin PL, Marques JP, et al. MP2RAGEME: T1, T2 *, and QSM mapping in one sequence at 7 Tesla. *Hum Brain Mapp*. 2018;40:1786–1798.
17. Sun H, Cleary JO, Glarin R, et al. Extracting more for less: multi-echo MP2RAGE for simultaneous T1 -weighted imaging, T1 mapping, R * 2 mapping, SWI, and QSM from a single acquisition. *Magn Reson Med*. 2020;83:1178–1191.
18. van der Zwaag W, Buur PF, Fracasso A, et al. Distortion-matched T1 maps and unbiased T1-weighted images as anatomical reference for high-resolution fMRI. *Neuroimage*. 2018;176:41–55.
19. Trotier AJ, Rapacchi S, Faller TL, et al. Compressed-sensing MP2RAGE sequence: application to the detection of brain metastases in mice at 7T. *Magn Reson Med*. 2018;81:551–559.
20. Mussard E, Hilbert T, Forman C, et al. Accelerated MP2RAGE imaging using Cartesian phyllotaxis readout and compressed sensing reconstruction. *Magn Reson Med*. 2020;84:1881–1894.
21. Hollingsworth KG, Higgins DM, McCallum M, et al. Investigating the quantitative fidelity of prospectively undersampled chemical shift imaging in muscular dystrophy with compressed sensing and parallel imaging reconstruction. *Magn Reson Med*. 2014;72:1610–1619.
22. Rovira A, Wattjes MP, Tintore M, et al. Evidence-based guidelines: MAGNIMS consensus guidelines on the use of MRI in multiple sclerosis-clinical implementation in the diagnostic process. *Nat Rev Neurol*. 2015;11:471–482.
23. Lustig M, Donoho D, Pauly JM. Sparse MRI: the application of compressed sensing for rapid MR imaging. *Magn Reson Med*. 2007;58:1182–1195.
24. Mazere J, Dilharreguy B, Catheline G, et al. Striatal and cerebellar vesicular acetylcholine transporter expression is disrupted in human DYT1 dystonia. *Brain*. 2021;144:909–923.
25. Tsuchida A, Laurent A, Crivello F, et al. The MRi-Share database: brain imaging in a cross-sectional cohort of 1870 university students. *Brain Struct Funct*. 2021;226:2057–2085. doi:10.1101/2020.06.17.154666.
26. Hansen MS, Sørensen TS. Gadgetron: an open source framework for medical image reconstruction. *Magn Reson Med*. 2013;69:1768–1776.
27. McKenzie CA, Yeh EN, Ohliger MA, et al. Self-calibrating parallel imaging with automatic coil sensitivity extraction. *Magn Reson Med*. 2002;47:529–538.
28. Beck A, Teboulle M. A fast iterative shrinkage-thresholding algorithm with application to wavelet-based image deblurring. *IEEE International Conference on Acoustics, Speech and Signal Processing*. 2009. doi:10.1109/ICASSP.2009.4959678.
29. Tustison NJ, Avants BB, Cook PA, et al. N4ITK: improved N3 bias correction. *IEEE Trans Med Imaging*. 2010;29:1310–1320. doi:10.1109/TMI.2010.2046908.
30. Manjón JV, Coupé P, Martí-Bonmatí L, et al. Adaptive non-local means denoising of MR images with spatially varying noise levels. *J Magn Reson Imaging*. 2010;31:192–203.
31. Manjón JV, Coupe P. volBrain: an online MRI brain volumetry system. *Front Neuroinform*. 2016;10:30.
32. Fujimoto K, Polimeni JR, van der Kouwe AJ, et al. Quantitative comparison of cortical surface reconstructions from MP2RAGE and multi-echo MPRAGE data at 3 and 7 T. *Neuroimage*. 2014;90:60–73.
33. Okubo G, Okada T, Yamamoto A, et al. MP2RAGE for deep gray matter measurement of the brain: a comparative study with MPRAGE. *J Magn Reson Imaging*. 2016;43:55–62.
34. Rioux JA, Levesque IR, Rutt BK. Biexponential longitudinal relaxation in white matter: characterization and impact on T1 mapping with IR-FSE and MP2RAGE. *Magn Reson Med*. 2016;75:2265–2277.
35. Dieringer MA, Deimling M, Santoro D, et al. Rapid parametric mapping of the longitudinal relaxation time T1 using two-dimensional variable flip angle magnetic resonance imaging at 1.5 tesla, 3 tesla, and 7 tesla. *PLoS One*. 2014;9:e91318.
36. Dezortova M, Lescinskij A, Dusek P, et al. Multiparametric quantitative brain MRI in neurological and hepatic forms of Wilson's disease. *J Magn Reson Imaging*. 2020;51:1829–1835.
37. Jutras JD, Wachowicz K, Gilbert G, et al. SNR efficiency of combined bipolar gradient echoes: comparison of three-dimensional FLASH, MPRAGE, and multiparameter mapping with VFA-FLASH and MP2RAGE. *Magn Reson Med*. 2017;77:2186–2202.
38. Preibisch C, Deichmann R. T1 mapping using spoiled FLASH-EPI hybrid sequences and varying flip angles. *Magn Reson Med*. 2009;62:240–246.

© 2022 The Author(s). Published by Wolters Kluwer Health, Inc.

39. Oros-Peusquens AM, Laurila M, Shah NJ. Magnetic field dependence of the distribution of NMR relaxation times in the living human brain. *MAGMA*. 2008;21: 131–147.
40. Gelman N, Ewing JR, Gorell JM, et al. Interregional variation of longitudinal relaxation rates in human brain at 3.0 T: relation to estimated iron and water contents. *Magn Reson Med*. 2001;45:71–79.
41. Wansapura JP, Holland SK, Dunn RS, et al. NMR relaxation times in the human brain at 3.0 tesla. *J Magn Reson Imaging*. 1999;9:531–538.
42. Weiskopf N, Suckling J, Williams G, et al. Quantitative multi-parameter mapping of R1, PD(*), MT, and R2(*) at 3T: a multi-center validation. *Front Neurosci*. 2013;7:95.
43. Palumbo L, Bosco P, Fantacci ME, et al. Evaluation of the intra- and inter-method agreement of brain MRI segmentation software packages: a comparison between SPM12 and FreeSurfer v6.0. *Phys Med*. 2019;64:261–272.
44. Droby A, Thaler A, Giladi N, et al. Whole brain and deep gray matter structure segmentation: quantitative comparison between MPRAGE and MP2RAGE sequences. *PLoS One*. 2021;16:e0254597.
45. Alonso J, Pareto D, Alberich M, et al. Assessment of brain volumes obtained from MP-RAGE and MP2RAGE images, quantified using different segmentation methods. *MAGMA*. 2020;33:757–767.
46. Alonso J, Pareto D, Alberich M, et al. Quantitative comparison of subcortical and ventricular volumetry derived from MPRAGE and MP2RAGE images using different brain morphometry software. *MAGMA*. 2021;34:903–914. doi:10.1007/s10334-021-00933-0.
47. Næss-Schmidt E, Tietze A, Blicher JU, et al. Automatic thalamus and hippocampus segmentation from MP2RAGE: comparison of publicly available methods and implications for DTI quantification. *Int J Comput Assist Radiol Surg*. 2016; 11:1979–1991.
48. Preibisch C, Deichmann R. Influence of RF spoiling on the stability and accuracy of T1 mapping based on spoiled FLASH with varying Flip angles. *Magn Reson Med*. 2009;61:125–135.
49. Deoni SC, Rutt BK, Peters TM. Rapid combined T1 and T2 mapping using gradient recalled acquisition in the steady state. *Magn Reson Med*. 2003;49: 515–526.
50. Feng L, Liu F, Soultanidis G, et al. Magnetization-prepared GRASP MRI for rapid 3D T1 mapping and fat/water-separated T1 mapping. *Magn Reson Med*. 2021;86: 97–114.
51. Wang X, Tan Z, Scholand N, et al. Physics-based reconstruction methods for magnetic resonance imaging. *Philos Trans A Math Phys Eng Sci*. 2021; 379:20200196.
52. Karakuzu A, Boudreau M, Duval T, et al. qMRLab: Quantitative MRI analysis, under one umbrella. *J Open Source Softw.* . 2020;5:2343. doi:10.21105/joss.02343.
53. Santos JM, Wright GA, Pauly JM. Flexible real-time magnetic resonance imaging framework. *Conf Proc IEEE Eng Med Biol Soc*. 2004;2:1048–1051.

© 2022 The Author(s). Published by Wolters Kluwer Health, Inc.